13

Materials Science and Engineering, A174 (1994) 165-171

Characterization of W–Me–C (Me = Fe, Co) films and their structural behaviour with temperature

B. Trindade and M. T. Vieira

Departamento de Engenharia Mecânica da Faculdade de Ciências e Tecnologia da Universidade de Coimbra, Largo D. Dinis, 3000 Coimbra (Portugal)

E. Bauer-Grosse

Laboratoire de Science et Génie des Surfaces, URA CNRS 1402, Ecole Nationale Supérieure des Mines, 54042 Nancy Cedex (France)

(Received December 8, 1992; in revised form June 22, 1993)

Abstract

Metastable W–Me–C (Me = Fe, Co) films were obtained by non-reactive RF magnetron sputtering. Their initial state and thermal stability were studied by means of electron probe microanalysis, secondary ion mass spectrometry and X-ray diffraction. The results show that the structure at room temperature depends on the percentage of iron and cobalt in the films, varying from β-WC$_{1-x}$ to amorphous with the increasing content of these elements. The structure of the crystalline films changes with temperature from β-WC$_{1-x}$ to WC and W$_2$C. The crystallization mechanism of the amorphous films is characterized by the formation of carbon-deficient phases, such as W$_2$C or M$_6$C.

1. Introduction

W–C-based films deposited by physical vapour deposition techniques are promising materials for tools. In previous work [1], W–Fe–C films were obtained by non-reactive RF diode sputtering and characterized at room temperature. Since integrity of a film component depends essentially on the adherence of the film to the substrate, significant structural changes with temperature, involving high internal stresses of both the film and substrate, must be avoided. The main objective of this work is the characterization of W–Me–C films deposited onto high-speed steel substrates by non-reactive RF magnetron sputtering and their structural transformations with temperature.

2. Experimental details

W–Me–C (Me = Fe, Co) films were obtained by sputtering WC + Co (0 at.% < Co < 15 at.%) targets partially covered by iron foils of different sizes. Films of 1 to 2 μm thickness were deposited onto quenched and tempered M2 (AISI) high-speed steel by non-reactive RF magnetron sputtering, at a deposition rate of 0.3 nm s^{-1} and an argon pressure of 1 Pa. Prior to the depositions, the substrates were sputter-cleaned at −1000 V for 5 min in an argon atmosphere.

The mean composition and the composition–depth profiles of the films were carried out by electron probe microanalysis (EPMA) and secondary ion mass spectrometry (SIMS) respectively. The structure of the films was examined by X-ray diffraction (XRD) using Co Kα radiation. For the analysis, an incidence angle of 4° was chosen in order to avoid the signals from the steel substrate.

The chemical and structural characterization of the W–Me–C films was performed before and after annealing. This heat treatment was carried out under vacuum (10^{-5} Pa) for 1 h at increasing temperatures. In order to avoid the ferrite to austenite transformation in steel, the highest annealing temperature attained in this work was 750 °C.

3. Experimental results

3.1. Chemical analysis

3.1.1. Electron probe microanalysis

The chemical composition of the as-deposited and treated W–Me–C films obtained by EPMA is summarized in Table 1. The results show an increasing iron

0921-5093/94/$7.00

TABLE 1. Atomic chemical composition of the targets and the W-Me-C (Me = Fe, Co) films in the as-deposition state and after annealing at 750 °C

Targets[a]	Reference	Coatings			
		As-deposited state		After annealing at 750 °C	
		Composition	M_xC	Composition	M_xC
(WC)	R1	$W_{56}C_{44}$	$M_{1.3}C$	$W_{63}C_{37}$	$M_{1.7}C$
$(WC)_{95}Co_5$ + Fe [~ 0.5 cm^2]	R2	$W_{47}Fe_4Co_{5.5}C_{43.5}$	$M_{1.3}C$	$W_{52}Fe_{5.5}Co_{7.5}C_{35}$	$M_{1.9}C$
(WC) + Fe [~ 0.5 cm^2]	R3	$W_{53}Fe_5C_{42}$	$M_{1.4}C$	$W_{58}Fe_6C_{36}$	$M_{1.8}C$
$(WC)_{95}Co_5$	R4	$W_{52}Co_6C_{42}$	$M_{1.4}C$	$W_{57}Co_7C_{36}$	$M_{1.8}C$
(WC) + Fe [~ 1 cm^2]	R5	$W_{46.5}Fe_{13}C_{40.5}$	$M_{1.5}C$	$W_{60}Fe_{12.5}C_{27.5}$	$M_{2.6}C$
$(WC)_{90}Co_{10}$	R6	$W_{48}Co_{13}C_{39}$	$M_{1.6}C$	$W_{59}Co_{13}C_{28}$	$M_{2.6}C$
$(WC)_{90}Co_{10}$ + Fe [~ 0.8 cm^2]	R7	$W_{43}Fe_7Co_{13}C_{37}$	$M_{1.7}C$	$W_{52}Fe_{8.5}Co_{16}C_{23.5}$	$M_{3.3}C$
$(WC)_{85}Co_{15}$ + Fe [~ 1 cm^2]	R8	$W_{38}Fe_{13}Co_{16}C_{33}$	$M_{2.0}C$	$W_{42}Fe_{15}Co_{17}C_{26}$	$M_{2.8}C$
(WC) + Fe [~ 3 cm^2]	R9	$W_{37}Fe_{30}C_{33}$	$M_{2.0}C$	$W_{42}Fe_{35}C_{23}$	$M_{3.3}C$
$(WC)_{85}Co_{15}$ + Fe [~ 2 cm^2]	R10	$W_{33}Fe_{20}Co_{15}C_{32}$	$M_{2.1}C$	$W_{39}Fe_{25}Co_{17}C_{18}$	$M_{3.4}C$
$(WC)_{95}Co_5$ + Fe [~ 2 cm^2]	R11	$W_{39}Fe_{24}Co_5C_{32}$	$M_{2.1}C$	$W_{42}Fe_{25}Co_6C_{27}$	$M_{2.7}C$
(WC) + Fe [~ 4 cm^2]	R12	$W_{31}Fe_{40}C_{29}$	$M_{2.4}C$	$W_{35}Fe_{47}C_{18}$	$M_{4.6}C$
$(WC)_{85}Co_{15}$ + Fe [~ 3 cm^2]	R13	$W_{27.5}Fe_{27}Co_{17.5}C_{28}$	$M_{2.6}C$	$W_{32}Fe_{33.5}Co_{17}C_{17.5}$	$M_{4.7}C$

[a] The atomic compositions of the WC-Co targets are those indicated by the manufacturer.

content in the films with an increase in the area of the iron foils used as targets in the co-sputtering process. The relative percentages of tungsten, cobalt and carbon in the films deviate slightly from those of the target, being partially enriched in the first two elements and depleted in the last one. All the films have W at.%/C at.% ratios higher than unity (except for R13), this ratio increasing with the decrease in iron and cobalt percentages.

After annealing at 750 °C, the carbon contents of the W-Me-C films are significantly lower than before heat treatment. The loss of carbon occurring during isothermal treatment is much more important the higher the initial atomic percentages of iron and cobalt in the films.

3.1.2. *Secondary ion mass spectrometry*

Figure 1 shows the C^-, O^-, Fe^+, Co^+ and W^+ SIMS sputter depth profiles obtained for the W-Me-C films in the as-deposited condition and after annealing at two different temperatures (650 °C and 750 °C). In this figure the counts of the secondary ions are plotted as a function of the distance to the surface.

For the as-deposited condition a well-defined film/substrate interface is observed at ~ 1.2 μm below the surface. Support for this view is gained from the fact that a decrease of the counts of the secondary C^-, Co^+ and W^+ ions is observed at that distance. A narrow oxygen peak is detected at the film/substrate interface which may be the result of oxygen impingement at the surface of the steel substrate.

The SIMS composition-depth profiles corresponding to annealing at 650 °C reveal the existence of diffusion phenomena from the film into the substrate and vice versa, and a less well-defined film/substrate interface. The intensity of the secondary C^- ions measured in the film is lower than that obtained before heat treatment. Moreover, a negative gradient of the C^- signal intensity is observed on the cross-section of the film, suggesting carbon diffusion into the substrate. The elements Co and W appear to diffuse from the film into the substrate while Fe diffuses in the opposite direction.

At an annealing temperature of 750 °C, the C^- ion signal becomes constant and of the same magnitude in the film and substrate. Cobalt and tungsten extend into the M2 substrate while iron diffuses into the film. All but the O^- profile now reveal a broad film/substrate interface.

3.2. *Structural analysis*

3.2.1. *X-ray diffraction*

The X-ray diffractograms obtained from as-deposited and heat-treated W-Me-C films show a clear dependence on chemical composition. Depending on the initial structure and structural changes occurring during heat treatment, they could be classified into four groups, Figs. 2(a)-2(d).

3.2.1.1. Group I. This group includes films without iron or cobalt (R1) with a crystalline structure in the as-deposited state. Their diffractograms show five relatively broad X-ray diffraction peaks ascribed to the NaCl-type β-WC_{1-x} phase [2]. The X-ray diffractograms obtained after annealing at 650 °C are quite similar to

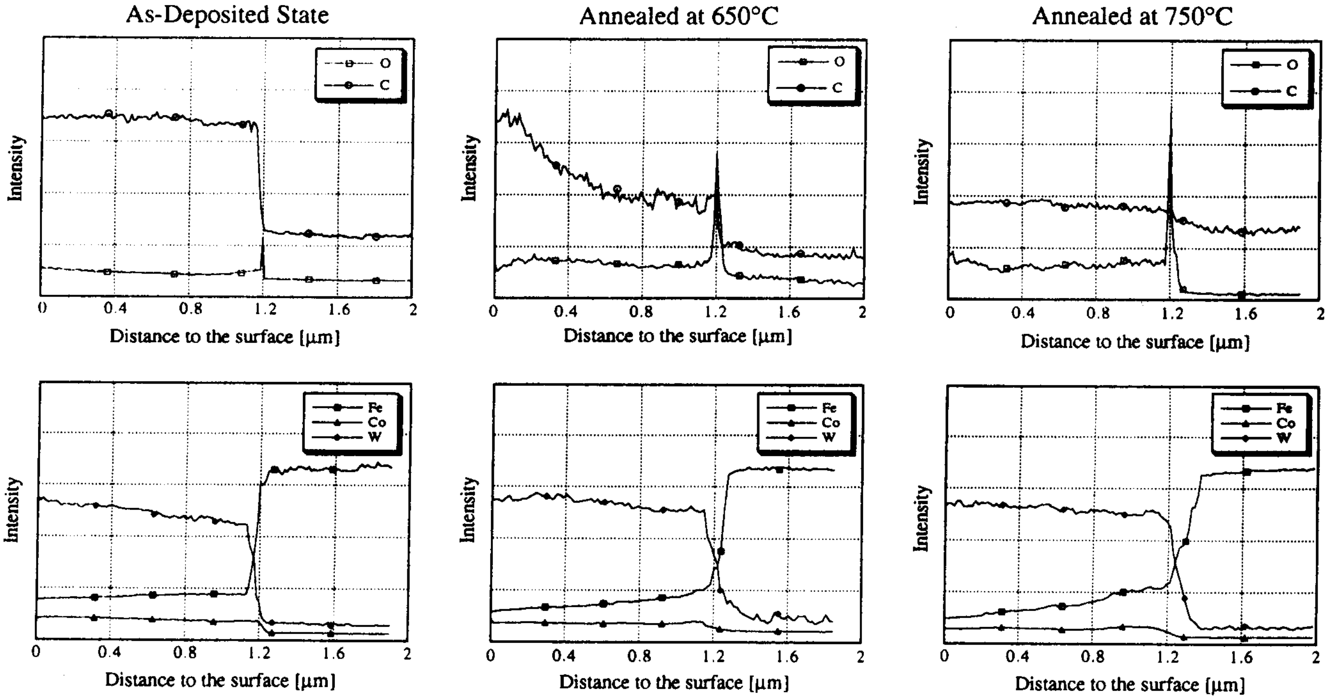

Fig. 1. SIMS sputter depth profiles for the film R10 on a M2 (AISI) high-speed steel substrate, in the as-deposited condition and after annealing at 650 °C and 750 °C.

those obtained for the as-deposited condition. However, the appearance of a very weak and broad peak at $2\theta = 57.26°$, corresponding to the $(10\bar{1}1)$ plane of the WC phase [3], should be pointed out. At 700 °C, a more pronounced $(10\bar{1}1)$ peak of WC and some broad peaks of W_2C [4] are visible. The (111) and (222) planes of the β-WC_{1-x} carbide show weaker intensities than before. The X-ray diffraction patterns obtained after annealing at 750 °C show a better definition of the peaks relating to the W_2C and WC phases and a weaker intensity of the (111) and (222) planes of the β-WC_{1-x} phase.

3.2.1.2. Group II. This group is constituted by films that before heat treatment have X-ray diffractograms revealing slight signs of crystallinity (R2, R3 and R4), with two broad diffraction peaks, characteristic of amorphous structures, and a third peak at $2\theta = 73.2°$, probably due to the (220) plane of the β-WC_{1-x} phase. The X-ray diffraction patterns obtained for annealing temperatures of 650 °C and 700 °C consist of five peaks ascribed to the β-WC_{1-x} phase in addition to a broad and weak sixth peak close to $2\theta = 57.1°$, indexed as the $(10\bar{1}1)$ plane of WC. The intensity of the $(10\bar{1}1)$ WC peak intensity increases with heat treatment temperature. X-ray diffraction patterns obtained for $T = 750$ °C show several well-defined W_2C peaks. No other peaks related to either the β-WC_{1-x} or the WC phase are visible for this annealing temperature.

3.2.1.3. Group III. This group contains films with X-ray diffractograms typical of amorphous structures, characterized by two broad diffraction peaks, and Me at.% lower than 40 (R5–R11). At $T = 650$ °C, fairly narrow peaks of W_2C may be observed in addition to these two broad peaks. Their intensity and definition seem to increase with the iron and cobalt contents in the films; the area under the two broad peaks of the amorphous phase decreases with an increase in the iron and cobalt content. For higher annealing temperatures, the X-ray diffractograms show peaks correlated to a crystalline two-phase structure of W_2C and M_6C [5]. Taking into account the intensity of the diffraction peaks obtained from the films of this group, it can be concluded that the relative final percentages of the W_2C and M_6C phases in these films depend on the total content of element Me. Coatings poorer in Fe and Co are essentially formed by W_2C while those richer in these elements by M_6C.

3.2.1.4. Group IV. This group includes amorphous as-deposited films with Me at.% higher than or equal to 40 (R12 and R13). In spite of the same initial structure, the phase transformations of these films with tempera-

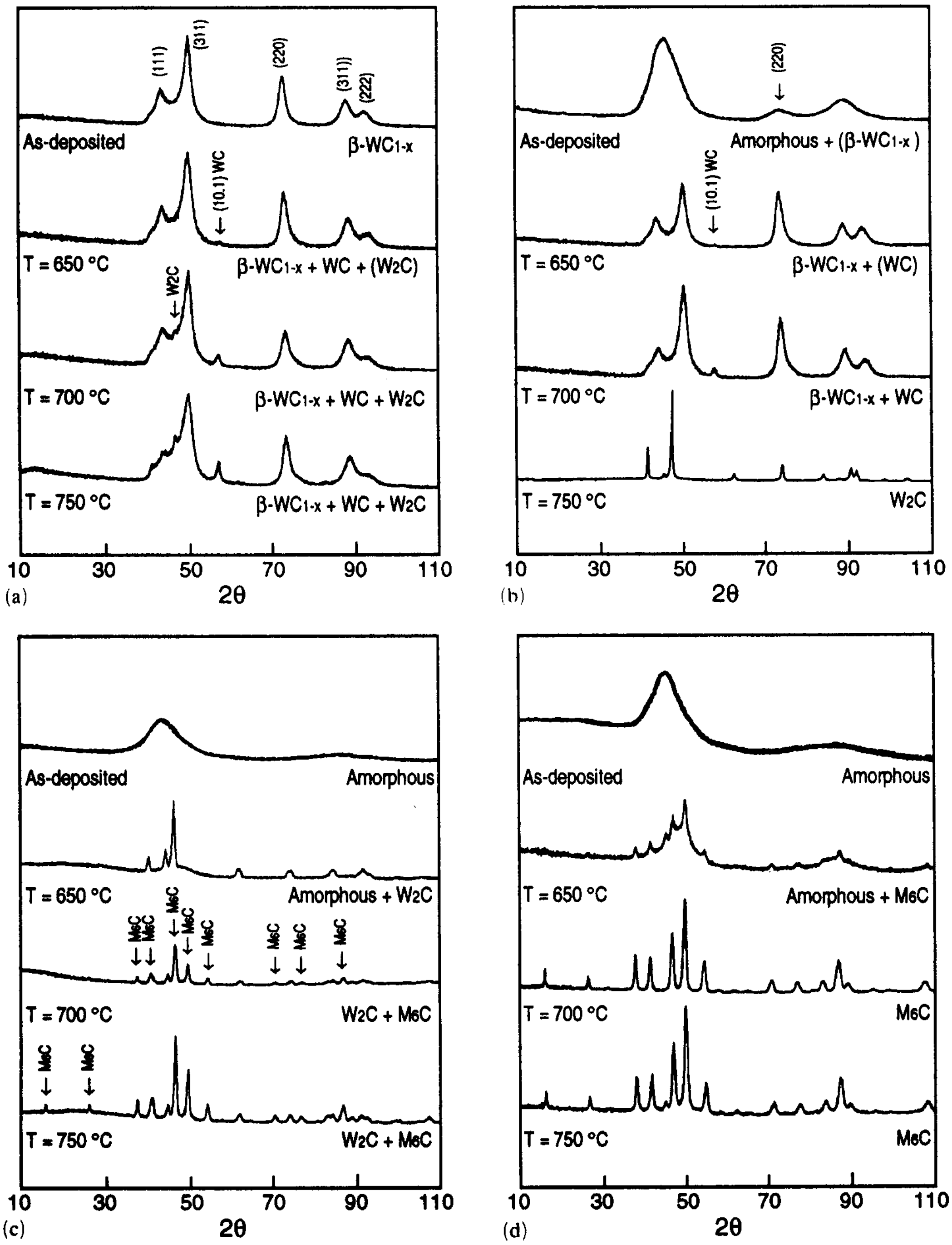

Fig. 2. X-ray diffraction patterns of the four groups of W-Me-C (Me = Fe, Co) films: (a) Group I; (b) Group II; (c) Group III; (d) Group IV.

ture are rather different from Group III films. Their structural evolution with temperature is characterized by the appearance of M_6C and the absence of W_2C.

4. Discussion

The chemical composition of as-deposited W-Me-C films deviate slightly from that of the targets, being partially enriched in tungsten and cobalt, and depleted in carbon. This can be interpreted in terms of the different sputtering yields for these three elements. In fact, despite the lower elemental sputtering yield of carbon relative to cobalt and tungsten [6] (for ion bombardment energies up to 1000 eV), for multicomponent materials a tendency for the lightest species to sputter preferentially has been predicted [7]. Thus, the film bombardment that occurs during the sputtering process leads to W–Me–C films richer in tungsten and cobalt and deficient in carbon.

The decrease of the W at.%/C at.% ratios observed with the increase in iron and cobalt percentages in the films is a direct consequence of a carbon sputtering yield dependence on the atomic weight of the nearest neighbours, as previously postulated by some authors [8–10] and later confirmed by H. F. Winters [11]. According to this author, nitrogen has a larger sputtering yield when its nearest neighbours are tungsten than when its nearest neighbours are molybdenum, as a consequence of mass effect. Thus, taking into account the similarities between the nitrogen and carbon atoms and the differences between the mass of W and the elements Fe and Co, it can be concluded that the carbon deficit in W–Me–C films is much more important the lower the iron and cobalt percentages in the targets.

Comparing the chemical composition of films in the as-deposited state and after annealing at 750 °C, it can be concluded that they lose carbon during heat treatment. Bearing in mind the characteristics of the carbon atom (interstitial type) and the different carbon percentages in the various films and M2 steel (~ 7.4 at.%), it is reasonable to accept that there is carbon diffusion into the substrate. A relationship between the initial composition of the films and the loss of carbon is observed, films richer in iron and cobalt (amorphous in the as-deposited state) being those that lose a larger amount of carbon during annealing. The diffusion of carbon may eventually be enhanced by a disordered environment induced by the difference between the atomic radii of both the iron and cobalt elements and that of tungsten, favouring the formation of structures poorer in carbon. Besides, since carbon has a higher affinity for tungsten than for iron or cobalt, lower activation energies should be necessary for carbon diffusion in films poorer in tungsten than for those richer in this element, favouring the migration of carbon atoms into the substrate.

X-ray diffraction analysis showed that the structure of as-deposited W–Me–C films is dependent on chemical composition. The results now obtained for the as-deposited state are comparable to those previously obtained for W–Fe–C [1] and W–Co–C [12] systems. In spite of the crystallinity signs of Group II films, only the $W_{56}C_{44}$ film (Group I) has a clear crystalline structure, indexed as β-WC_{1-x} [2]. This carbide has an NaCl-type structure, and is believed to be a cubic variant of WC [13]. When obtained by conventional methods, β-WC_{1-x} is a high temperature phase and exists only above 2530 °C [14]. Its occurrence in the as-deposited state of sputtered W–Me–C crystalline film is not in agreement with the W–C equilibrium diagram [14] but is in accordance with the M-to-C initial ratios (1.3–1.4). Films richer in iron and cobalt (Groups III and IV) in the as-deposited state present X-ray diffractograms with two broad peaks, characteristic of amorphous materials. In fact, their widths indicate, by the Sherrer equation [15], particle sizes below 1.5 nm, which implies short distance order [16]. A parallel study that we have undertaken on these films [17] by means of transmission electron microscopy has shown bright field images without contrast and associated electron diffraction patterns with very broad and diffuse rings confirming the existence of amorphous structures. In the literature of W–Me–C sputtered films, there are some references to amorphous structures [1, 12, 18–21]. Among the possible explanations of these two elements contributing to the amorphization of W–Me–C films, the most plausible are:

(1) The melting temperature decreases and T_g increases in W–Me–C systems with increasing iron and cobalt content. This idea was advanced for the W–Co–C system by Cavaleiro [12] on the basis of the work of Takayama [16] and Chen [22], for the Pd–Co–Si system.

(2) Low solubility of iron and cobalt in the W–Me–C systems prevents the formation of supersaturated solid solutions. In fact, in a previous study concerning the influence of iron on the structure of W–Fe–C as-deposited films obtained by non-reactive RF diode sputtering [1], we showed that for low iron concentrations it was possible to obtain crystallinity. By means of XRD and Mössbauer spectroscopy it was concluded that for up to 9 at.%, iron atoms substitute those of tungsten in the f.c.c. lattice of the β-WC_{1-x} phase. Above this value they cannot replace the atoms of tungsten in such a structure and the films become amorphous.

The thermal behaviour of W–Me–C films obtained in this work showed structural changes with temperature, the type of phase transformations and the final structure of the films being dependent on their initial composition. As previously mentioned, the structure of crystalline as-deposited films changes with temperature from β-WC_{1-x} to the less compact structures WC and W_2C, which can be understood by the higher low-temperature stabilities of these last two structures when compared to that of the first. In the W–C equilibrium diagram, WC exists as a single phase from room temperature up to 2776 °C, while W_2C exists within a narrow range of 30 at.% and is capable of appearing in three states [13, 14], depending on the temperature:

(a) α-(W_2C), an ordered hexagonal or pseudohexagonal structure stable between 1250 °C and 2100 °C;
(b) β-(W_2C), an orthorhombic phase (Fe_2N-type) existing in the range 2100–2400 °C;
(c) γ-(W_2C), a disordered hexagonal structure stable

between 2450 °C and the melting point. It was not possible in this study to ascribe the W_2C phase to one of the three crystallographic structures, α-(W_2C), β-(W_2C) or γ-(W_2C), due to their similar interplanar distances [4].

The crystallization mechanism of Group II films is characterized by the formation of WC from the as-deposited structure and later by the development of W_2C. Judging from the metastability of the β-WC_{1-x} phase, one may accept that this carbide already exists before annealing (as-deposited state), in an embryonic state, as previously suggested. If this assumption is true, there is no amorphous to β-WC_{1-x} transformation but only an increase in the β-WC_{1-x} particle size with temperature. The W_2C formation from β-WC_{1-x} and WC is in accordance with the carbon impoverishment of these films during successive annealing heat treatments (Table 1). The final M-to-C ratios obtained for films of Group II (1.8–1.9) are consistent with the existence of a W_2C single phase and suggest a certain solubility of iron and cobalt in this carbide.

For Group III films, the W_2C carbide is the first crystalline structure that occurs with increasing annealing temperature. This may be explained by the initial deficit in carbon of these films (1.5–2.1) that does not allow the formation of phases richer in carbon (WC and β-WC_{1-x}). The M_6C carbide (cubic carbide, with M = W, Fe and Co) is the final structure to appear and it is quite difficult to know if it comes directly from the amorphous phase or if it is the result of a structural transformation of W_2C into M_6C in a matrix enriched in iron and cobalt. It seems that M_6C grows predominantly from the W_2C phase, as observed in tungsten alloyed steels [23]. In fact, the structural stability of the M_6C phase [24] at high temperatures and the similarity of carbon atoms in both structures favour the W_2C to M_6C structural transformation. The loss of carbon necessary for the formation of M_6C from W_2C is due to the increase of carbon diffusion into the substrate with annealing temperature. As stated above, for this set of W–Me–C films, W_2C is the dominant phase in those with low iron and cobalt content, while M_6C is the major phase in those richer in these two elements. The mean compositions of these heat-treated films oscillate from $M_{2.6}C$ (R5) to $M_{3.4}C$ (R10), which is in agreement with the simultaneous presence of $W_2C + M_6C$.

The structural evolution with temperature of Group IV films, as opposed to the other W–Me–C films, is characterized by the absence of β-WC_{1-x}, WC and W_2C phases. The M_6C phase is formed from the amorphous matrix. This behaviour is explained by the higher content of iron and cobalt in the structure of W–Me–C films. As mentioned above, the increased Me content in the amorphous structure favours the decrease of carbon in the film during heat treatment.

5. Conclusions

The results of a structural characterization study of sputtered W–Me–C (Me = Fe, Co) films in the as-deposited state and after annealing at increasing temperatures have been reported. The following conclusions may be drawn from this study:

(1) The structure of the as-deposited films is dependent on chemical composition; it changes from β-WC_{1-x} to amorphous with increasing iron and cobalt contents.

(2) The thermal structural evolution of the W–Me–C films essentially depends on the Me percentage. During annealing, the sequence of structural transformations with increasing Me and temperature is $\beta\text{-}WC_{1-x} \rightarrow WC \rightarrow W_2C \rightarrow M_6C$.

(3) Both SIMS and EPMA measurements showed carbon diffusion into the steel substrates for all W–Me–C films during successive heat treatments. This means that the application of W–Me–C films deposited onto steel as hard films for tools may require the existence of an additional layer between the film and substrate to act as a barrier to the migration of carbon atoms into the steel substrate. Another solution might be the incorporation of another element in the W–Me–C films that would stabilize the as-deposited structure and would avoid the diffusion of carbon into the steel.

Acknowledgments

Sponsorship for one of the authors by the Junta Nacional de Investigação Científica, given in the framework of a Portuguese–French research network, is gratefully acknowledged.

References

1 B. Trindade and M. T. Vieira, *Thin Solid Films, 206* (1991) 318.
2 Joint Committee on Powder Diffraction File, International Center for Powder Diffraction Data, Swarthmore, PA, Card 20-1316.
3 Joint Committee on Powder Diffraction File, International Center for Powder Diffraction Data, Swarthmore, PA, Card 25-1047.
4 Joint Committee on Powder Diffraction File, International Center for Powder Diffraction Data, Swarthmore, PA, Cards 20-1315, 31-1408 and 35-776.
5 Joint Committee on Powder Diffraction File, International Center for Powder Diffraction Data, Swarthmore, PA, Card 3-980.
6 R. V. Stuart and G. K. Wehner, *J. Appl. Phys., 33* (1962) 2345.

7 P. Sigmund, Sputtering by particle bombardment, in R. Behrisch (ed.), *Topics in Applied Physics*, Springer, Berlin, 1981, p. 10.
8 P. K. Haff, *Appl. Phys. Lett., 31* (1977) 259.
9 Z. L. Liau, W. L. Brown, R. Homer and J. M. Poate, *Appl. Phys. Lett., 30* (1977) 626.
10 R. Kelly, *Surf. Sci., 100* (1980) 85.
11 H. F. Winters, *J. Vac. Sci. Technol., 3* (1982) 493.
12 A. Cavaleiro, M. T. Vieira and G. Lemperière, *Thin Solid Films, 197* (1991) 237.
13 E. Rudy and S. T. Windisch, *J. Am. Ceram. Soc., 50* (5) (1967) 272.
14 G. V. Raynor and V. G. Rivlin, *Phase Equilibria in Iron Ternary Alloys*, The Institute of Metals, London, 1988, p. 25.
15 A. Guinier, *Theorie et Technique de la Radiocristalographie*, Dunod, Paris, 1956, p. 462.
16 S. Takayama, *J. Mater. Sci., 11* (1976) 164.
17 B. Trindade, M. T. Vieira and E. Bauer-Grosse, submitted to *Acta Metall. Mater.*
18 K. Fuchs, P. Rodhammer, A. Tschulik, K. Kailer, R. Weirather, E. Bertel and F. P. Netzer, *11th Int. Plansee Seminar 85, Metallwerk Plansee, Reutte*, 1985, p. 207.
19 K. Fuchs, P. Rodhammer, E. Bertel, F. P. Netzer and E. Gornik, *International Symposium on Trends and New Applications in Thin Films, Strasbourg*, 1987, p. 587.
20 K. Fuchs, P. Rodhammer, E. Bertel, F. P. Netzer and E. Gornik, *Thin Solid Films, 151* (1987) 383.
21 K. Machida, M. Enyo and I. Toyoshima, *Thin Solid Films, 161* (1988) 191.
22 H. S. Chen, *Acta Metall., 22* (1974) 1505.
23 H. Fredriksson, M. Hillert and M. Nica, *Scand. J. Metall., 8* (1979) 115.
24 H. J. Goldschmidt, *J. Iron Steel Int.*, December (1948) 345.